Applied Microscopy
Korean Society of Microscopy

pISSN 2287-5123 · eISSN 2287-4445
http://dx.doi.org/10.9729/AM.2012.42.4.207

Synthesis and Characterization of a Pt/NiO/Pt Heterostructure for Resistance Random Access Memory

Hyung-Kyu Kim[1,2], Jee-Hwan Bae[1], Tae-Hoon Kim[1], Kwan-Woo Song[1], Cheol-Woong Yang[1,*]

[1]School of Advanced Materials Science and Engineering, Sungkyunkwan University, Suwon 440-746, Korea
[2]Coating Technology Team, Doosan Technical Center, Yongin 448-795, Korea

*Correspondence to:
Yang CW,
Tel: +82-31-290-7362
Fax: +82-31-290-7371
E-mail: cwyang@skku.edu

Received November 19, 2012
Revised December 6, 2012
Accepted December 6, 2012

We examined the electrical properties and microstructure of NiO produced using a sol-gel method and Ni nitrate hexahydrate ($Ni[NO_3]_2 \cdot 6H_2O$) to investigate if this NiO thin film can be used as an insulator layer for resistance random access memory (ReRAM) devices. It was found that as-prepared NiO film was polycrystalline and presented as the nonstoichiometric compound $Ni_{1+x}O$ with Ni interstitials (oxygen vacancies). Resistance-switching behavior was observed in the range of 0~2 V, and the low-resistance state and high-resistance state were clearly distinguishable (~10^3 orders). It was also demonstrated that NiO could be patterned directly by KrF eximer laser irradiation using a shadow mask. NiO thin film fabricated by the sol-gel method does not require any photoresist or vacuum processes, and therefore has potential for application as an insulating layer in low-cost ReRAM devices.

Key Words: Resistance-switching, Resistance random access memory, NiO, Laser decomposition, Sol-gel method

INTRODUCTION

As conventional flash memories approach their physical scalability limits, a great amount of research effort has been focused on next generation memory devices. Resistance random access memory (ReRAM) has attracted considerable interest due to its simple metal-insulator-metal structure and very fast access time. Resistance-switching behaviors have been observed in various oxide materials, such as binary oxides (ZrO_2, HfO_2, Fe_2O_3, and NiO), doped $Pr_{1-x}Ca_xMnO_3$ (PCMO), and doped perovskite materials (Cr-doped $SrTiO_3$) (Gibbons & Beadle, 1964; Beck et al., 2000; Zhuang et al., 2002; Seo et al., 2004; Park et al., 2007; Inoue et al., 2008; Guan et al., 2009). In particular, NiO has been widely studied since Gibbons & Beadle (1964) discovered bi-resistance states of NiO thin film after the electrical forming process. NiO thin film also has the advantages of simple components, less sensitivity to the structural phase, and a high ratio of on-off resistance states (Seo et al., 2004; Seo et al., 2005; Kim et al., 2006).

Ni oxide films are conventionally deposited or grown by reactive sputtering, pulsed laser deposition, or thermal oxidation (Ishihara et al., 2008; Chang et al., 2009; Liu et al., 2009). In comparison to these conventional techniques, the sol-gel method has the advantages of being both cheaper and simpler. In addition, $Ni(NO_3)_2 \cdot 6H_2O$ can easily be patterned and transformed into Ni oxide by laser beam irradiation, and unexposed Ni nitrate can be removed using deionized (DI) water (Park et al., 2011). This method uses the same type of optical modulation as conventional lithography, but does not require any photoresist or vacuum processes. This method is not only compatible with low-temperature and large-area fabrication, it also requires significantly fewer processing steps than conventional lithographic patterning technology.

This work was supported by the National Research Foundation of Korea (NRF) grants funded by the Korea Government (MEST) (No. 2011-0017257, No. 2011-0019984 and No. 2011-0030803).

In this study, we examined the resistance-switching properties and microstructure of NiO formed by a sol-gel method using $Ni(NO_3)_2 \cdot 6H_2O$ to evaluate the suitability of the resultant NiO thin films for ReRAM devices.

MATERIALS AND METHODS

To fabricate the Pt/NiO/Pt heterostructure, approximately 10 nm-thick Ti and 50 nm-thick Pt films were deposited as a bottom electrode on *p*-type (100) Si substrates using a DC magnetron sputtering system at room temperature. The base pressure was 6×10^{-7} Torr and the deposition pressure during the sputtering was 3 mTorr with Ar gas. During the deposition process, the power was 100 W for 299 seconds. A Ti layer was deposited as a buffer layer to improve adhesion between the Pt electrode and the Si substrate. A 0.2 M Ni nitrate solution was prepared by dissolving $Ni(NO_3)_2 \cdot 6H_2O$ (Sigma-Aldrich Inc., St Louis, MO, USA) in ethanol. Polyvinyl-pyrrolidone (PVP) was added into the solution to increase the wettability between the Pt bottom electrode and the Ni nitrate film (Bahari Molla Mahaleh et al., 2008). Spin-coating was used at 300 rpm for 5 minutes to deposit uniform Ni nitrate thin films on the Pt/Ti/Si substrate. Then, the Ni nitrate-coated Pt/Ti/Si substrate was exposed to a KrF excimer laser (λ=248 nm, 30 ns, 5 Hz) in air using a circular shadow mask with 150 μm diameter for 3 minutes. After laser irradiation, unexposed Ni nitrate was removed by DI water. Finally, Pt film was deposited as a top electrode by magnetron sputtering. The microstructure and chemical composition of the resultant thin films were assessed using a scanning electron microscope (SEM) (XL40FEG; Philips Co., Ltd., Eindhoven, The Netherlands) and a transmission electron microscope (TEM) (JEM-2100F; JEOL Co., Ltd., Tokyo, Japan) equipped with a scanning transmission electron microscope (STEM)/energy dispersive X-ray spectrometer (EDS). Cross-sectional TEM specimens were prepared using a focused ion beam (FIB) (SMI-3050TB; SII Nanotechnology Inc., Chiba, Japan). The surface morphology of Ni nitrate film that had been exposed to the KrF excimer laser and rinsed with DI water was measured by high-resolution atomic force microscopy (HR-AFM) (SPA-300HV; SII Nanotechnology Inc.). The current-voltage (*I-V*) characteristics of the fabricated devices were analyzed using a DC probe station (HP 4145B; Agilent Technologies Inc., Santa Clara, CA, USA) at room temperature under normal atmospheric conditions. During *I-V* measurements, the bottom electrode was grounded and a bias voltage was applied to the top electrode.

RESULTS AND DISCUSSION

Fig. 1 shows SEM images of an array of NiO patterned onto laser-exposed areas of a Ni nitrate-coated Pt/Ti/Si substrate. The brighter contrast circular regions (see Fig. 1A) are Ni oxides patterned by KrF laser irradiation for 3 min followed by the removal of unexposed Ni nitrate by DI water; the size of the area converted to NiO was approximately 150 μm in diameter. Fig. 1B shows the edge of the NiO circular pattern; the upper area of the image was not exposed to laser while the lower area was exposed to a KrF excimer laser (marked in Fig. 1B). EDS mapping as shown in the inset of Fig. 1B was carried out to determine the elemental distribution and to validate the patterning process. After KrF excimer laser irradiation, Ni nitrate may not be entirely transformed into NiO; Ni salt may potentially be present. However, nitrogen was not detected by

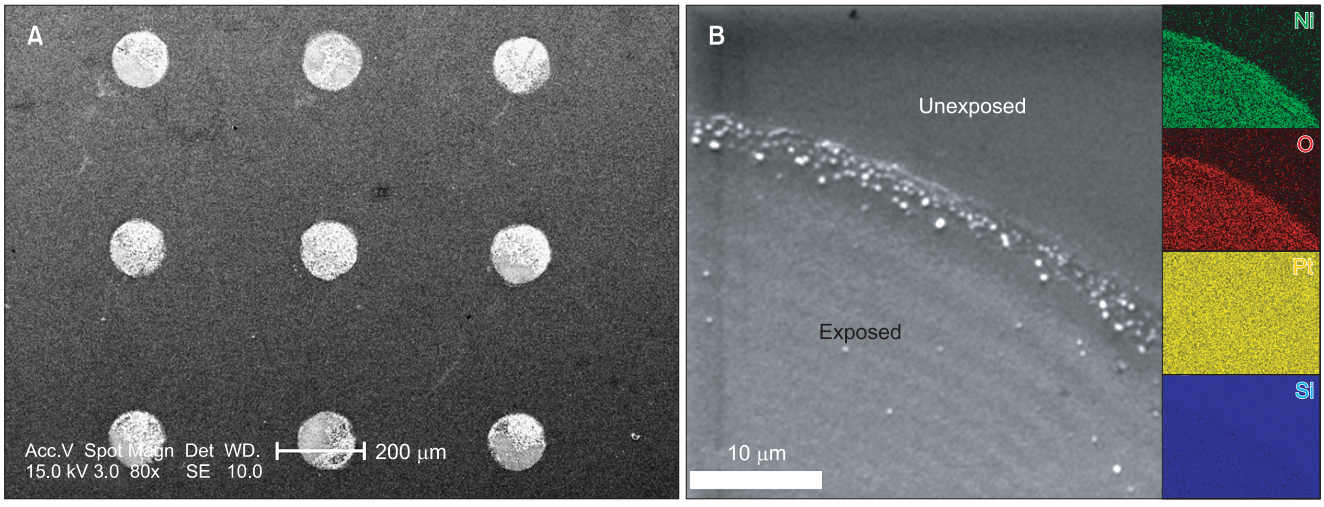

Fig. 1. SEM images of patterned Ni oxide after KrF excimer laser irradiation. (A) A low magnification image of the array of patterned NiO in the shape of a circle with a diameter of 150 μm, and (B) high magnification of the edge of a circular pattern and EDS maps of the elements Ni, O, Pt, and Si. SEM, scanning electron microscope; EDS, energy dispersive X-ray spectrometer.

EDS. These maps clearly demonstrated that the unexposed Ni nitrate was successfully removed by DI water and that the exposed region was composed of Ni and O atoms. These results are similar to our previous work (Park et al., 2011) and those reported for a negative photoresist process. The transformation mechanism was likely laser-induced thermal decomposition of $Ni(NO_3)_2 \cdot 6H_2O$. It has been reported that the thermal decomposition of $Ni(NO_3)_2 \cdot 6H_2O$ to produce NiO involves several reaction steps including many intermediate phases (Brockner et al., 2007). However, detailed information about the reaction steps and intermediate phases is not important in the context of this study, because our focus was the final NiO product. In addition, PVP, which was added into the solution to increase the wettability of the Pt surface, can be removed easily at 200°C (Park et al., 2011).

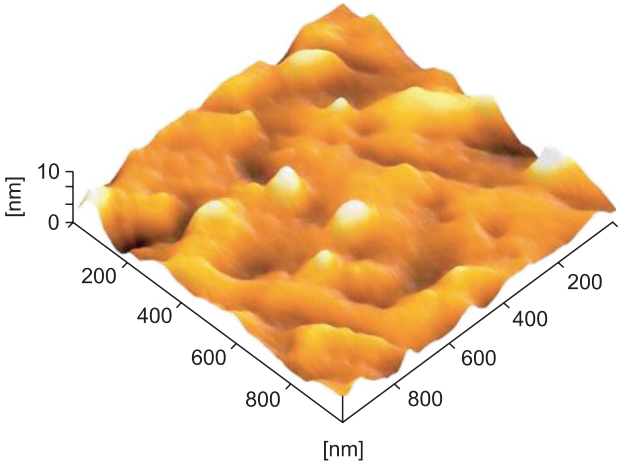

Fig. 2. HR-AFM image of the surface of the NiO film after KrF excimer laser irradiation. The scan area is 1×1 μm. HR-AFM, high-resolution atomic force microscopy.

An HR-AFM image of the surface of NiO film after KrF excimer laser irradiation is shown in Fig. 2; the scanning area is a 1×1 μm square. The root mean square (RMS) was measured to be 1.515 nm. This value is similar to that reported for NiO films deposited by the sputtering method (Kim et al., 2009).

The microstructure and chemical composition of the Pt/NiO/Pt heterostructure were examined by a TEM equipped with a STEM/EDS. Fig. 3 shows TEM micrographs of the fabricated device along with the nano-beam electron diffraction (NBED) pattern obtained from the Ni oxide layer. The thickness of the Ni oxide layer was about 50 nm (see Fig. 3A). As shown in the HR-TEM micrograph (see Fig. 3B), the Ni oxide layer transformed from Ni nitrate film by KrF excimer laser exposure had a polycrystalline structure, but the Ni oxide grains did not have a uniform size. The NBED pattern in the inset of Fig. 3B, which was obtained from a Ni oxide grain, was indexed as the [101] zone axis pattern of NiO, which has

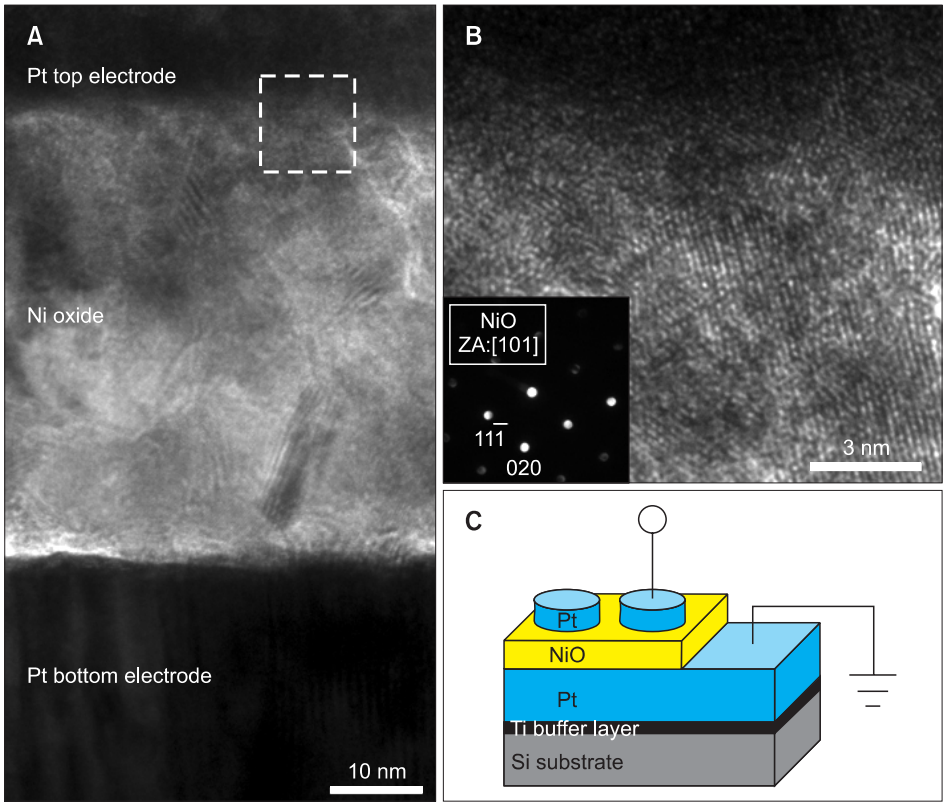

Fig. 3. (A) Cross-sectional TEM micrograph of the Pt/NiO/Pt heterostructure, (B) HR-TEM micrograph of the marked area in (A) and NBED pattern obtained from the NiO grain (inset), and (C) schematic diagram of the specimen and the overall circuit arrangement used to measure the *I-V* characteristics of the thin film. TEM, transmission electron microscope; HR, high-resolution; NBED, nano-beam electron diffraction.

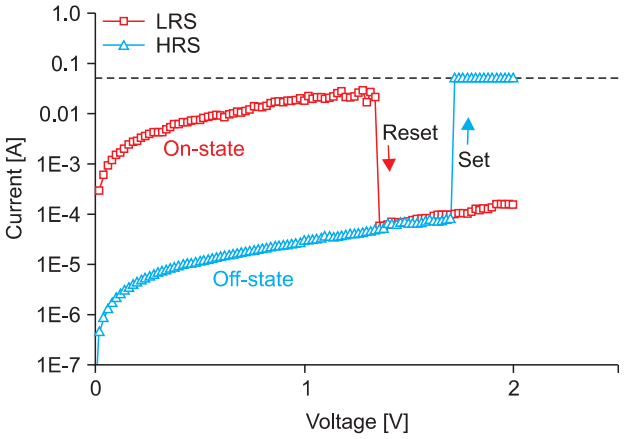

Fig. 4. Resistance-switching characteristics of the Pt/NiO/Pt heterostructure. Squares represent the on-state (low-resistance state, LRS) and the reset voltage was about 1.35 V. Triangles represent the off-state (high-resistance state, HRS) and the set voltage was about 1.71 V. The y-axis shows current on a logarithmic scale. The dashed horizontal line represents the setting limit of the current flow.

an fcc structure with a=4.1771 Å. The STEM/EDS results for the NiO grain were 55.25±1.03 at.% Ni and 44.75±3.76 at.% O. Natural NiO is a well-known metal-deficient *p*-type semiconductor; however, in this experiment, $Ni_{1+x}O$ was determined to be the Ni-rich phase.

To examine the resistance-switching properties and to evaluate the applicability of the as-prepared NiO films in ReRAM devices, we took *I-V* measurements. The NiO thin films displayed typical unipolar *I-V* characteristics of a Pt/NiO/Pt heterostructure (Fig. 4). The top electrode was patterned to be 150 μm in diameter using a metal shadow mask (see Fig. 3C). The current was measured by a tungsten tip on the top electrode in single-sweep mode and voltage was applied in the range of 0~2 V with a step of 0.02 V. The compliance current was limited to 50 mA (marked dash line in Fig. 4). When the applied voltage reached at 1.35 V, the current dropped suddenly and the cell had a high-resistance state (HRS; off-state, open-triangle and blue line in Fig. 4). When the applied voltage reached at 1.71 V, the current increased abruptly and the cell had a low-resistance state (LRS; on-state, open-square and red line in Fig. 4). If a specific voltage was applied only once, the resistance state remained constant until the voltage changed. The resistance of HRS was nearly three orders of magnitude greater than that of LRS in the range of 0~1 V, which is a sufficient interval to sense bistable resistance states. The mechanism of this resistance-switching behavior has not been clarified, but several hypotheses such as rupture or formation of conducting filaments and generation of a Schottky barrier at the interface have been posed (Sawa et al., 2005; Kim et al., 2009; Waser et al., 2009). In particular, it has been reported that the resistance-switching mechanism of NiO may be based on rupture or formation of conducting filaments at certain voltages with these electrical paths created by oxygen vacancies (Ni interstitials) (Kim et al., 2009). Moreover, Seo et al. (2005) reported that the more Ni interstitials present in a NiO film, the better the resistance-switching properties of the film.

SUMMARY

We examined the resistance-switching properties and microstructure of NiO films formed from $Ni(NO_3)_2 \cdot 6H_2O$ using a sol-gel method and directly patterned by KrF excimer laser irradiation. The NiO film was polycrystalline and comparatively homogeneous. The Pt/NiO/Pt heterostructure showed different resistance values depending on the applied voltage, and the difference between the LRS and HRS states was on the order of 10^3. This performance is comparable to that of existing ReRAM prepared by other processes. Therefore, sol-gel-derived NiO film can potentially be used in the production of low-cost ReRAM devices.

ACKNOWLEDGMENTS

The authors gratefully appreciate technical support from the cooperative center for research facilities (CCRF) at Sungkyunkwan University.

REFERENCES

Bahari Molla Mahaleh Y, Sadrnezhaad S K, and Hosseini D (2008) NiO nanoparticles synthesis by chemical precipitation and effect of applied surfactant on distribution of particle size. *J. Nanomater.* **2008**, 470595.

Beck A, Bednorz J G, Gerber C, Rossel C, and Widmer D (2000) Reproducible switching effect in thin oxide films for memory applications. *Appl. Phys. Lett.* **77**, 139-141.

Brockner W, Ehrhardt C, and Gjikaj M (2007) Thermal decomposition of nickel nitrate hexahydrate, $Ni(NO_3)_2 \cdot 6H_2O$, in comparison to $Co(NO_3)_2 \cdot 6H_2O$ and $Ca(NO_3)_2 \cdot 4H_2O$. *Thermochim. Acta.* **456**, 64-68.

Chang S H, Lee J S, Chae S C, Lee S B, Liu C, Kahng B, Kim D W, and Noh T W (2009) Occurrence of both unipolar memory and threshold resistance switching in a NiO film. *Phys. Rev. Lett.* **102**, 026801.

Gibbons J F and Beadle W E (1964) Switching properties of thin NiO films. *Solid-State Electron.* **7**, 785-797.

Guan W, Long S, Hu Y, Liu Q, Wang Q, and Liu M (2009) Resistance switching characteristics of zirconium oxide containing gold nanocrystals for nonvolatile memory applications. *J. Nanosci.*

Nanotechnol. **9**, 723-726.

Inoue I H, Yasuda S, Akinaga H, and Takagi H (2008) Nonpolar resistance switching of metal/binary-transition-metal oxides/metal sandwiches: homogeneous/inhomogeneous transition of current distribution. *Phys. Rev. B* **77**, 035105.

Ishihara T, Ohkubo I, Tsubouchi K, Kumigashira H, Joshi U S, Matsumoto Y, Koinuma H, and Oshima M (2008) Electrode dependence and film resistivity effect in the electric-field-induced resistance-switching phenomena in epitaxial NiO films. *Mater. Sci. Eng. B* **148**, 40-42.

Kim C H, Moon H B, Min S S, Jang Y H, and Cho J H (2009) Nanoscale formation mechanism of conducting filaments in NiO thin films. *Solid State Commun.* **149**, 1611-1615.

Kim D C, Seo S, Ahn S E, Suh D S, Lee M J, Park B H, Yoo I K, Baek I G, Kim H J, Yim E K, Lee J E, Park S O, Kim H S, Chung U, Moon J T, and Ryu B I (2006) Electrical observations of filamentary conductions for the resistive memory switching in NiO films. *Appl. Phys. Lett.* **88**, 202102.

Liu C, Chae S C, Lee J S, Chang S H, Lee S B, Kim D W, Jung C U, Seo S, Ahn S E, Kahng B, and Noh T W (2009) Abnormal resistance switching behaviours of NiO thin films: possible occurrence of both formation and rupturing of conducting channels. *J. Phys. D: Appl. Phys.* **42**, 015506

Park I S, Lee J H, Lee S W, and Ahn J H (2007) Resistance switching characteristics of HfO_2 film with electrode for resistance change random access memory. *J. Nanosci. Nanotechnol.* **7**, 4139-4142.

Park M H, Lee J W, Lee Y I, Lee J H, Hwang J H, Kim H K, and Yang C W (2011) Patterning of catalysts for the selective growth of carbon nanotubes using laser irradiation of nickel nitrate. *J. Nanosci. Nanotechnol.* **11**, 602-605.

Sawa A, Fujii T, Kawasaki M, and Tokura Y (2005) Interface transport properties and resistance switching in perovskite-oxide heterojunctions. *Proc. SPIE* **5932**, 59322C.

Seo S, Lee M J, Kim D C, Ahn S E, Park B H, Kim Y S, Yoo I K, Byun I S, Hwang I R, Kim S H, Kim J S, Choi J S, Lee J H, Jeon S H, Hong S H, and Park B H (2005) Electrode dependence of resistance switching in polycrystalline NiO films. *Appl. Phys. Lett.* **87**, 263507.

Seo S, Lee M J, Seo D H, Jeoung E J, Suh D S, Joung Y S, Yoo I K, Hwang I R, Kim S H, Byun I S, Kim J S, Choi J S, and Park B H (2004) Reproducible resistance switching in polycrystalline NiO films. *Appl. Phys. Lett.* **85**, 5655.

Waser R, Dittmann R, Staikov G, and Szot K (2009) Redox-based resistive switching memories - nanoionic mechanisms, prospects, and challenges. *Adv. Mater.* **21**, 2632-2663.

Zhuang W W, Pan W, Ulrich B D, Lee J J, Stecker L, Burmaster A, Evans D R, Hsu S T, Tajiri M, Shimaoka A, Inoue K, Naka T, Awaya N, Sakiyama A, Wang Y, Liu S Q, Wu N J, and Ignatiev A (2002) Novell colossal magnetoresistive thin film nonvolatile resistance random access memory (RRAM). In: *Electron Devices Meeting, 2002.* IEDM '02. International, pp. 193-196, (IEEE Conference Publications, Piscataway).